Electronic Supplementary Material (ESI) for Physical Chemistry Chemical Physics.

1 Supplementary Information

1.1 PXRD

This section provides the full PXRD temperature measurements made from 13–298 K on the quinacridone solids.

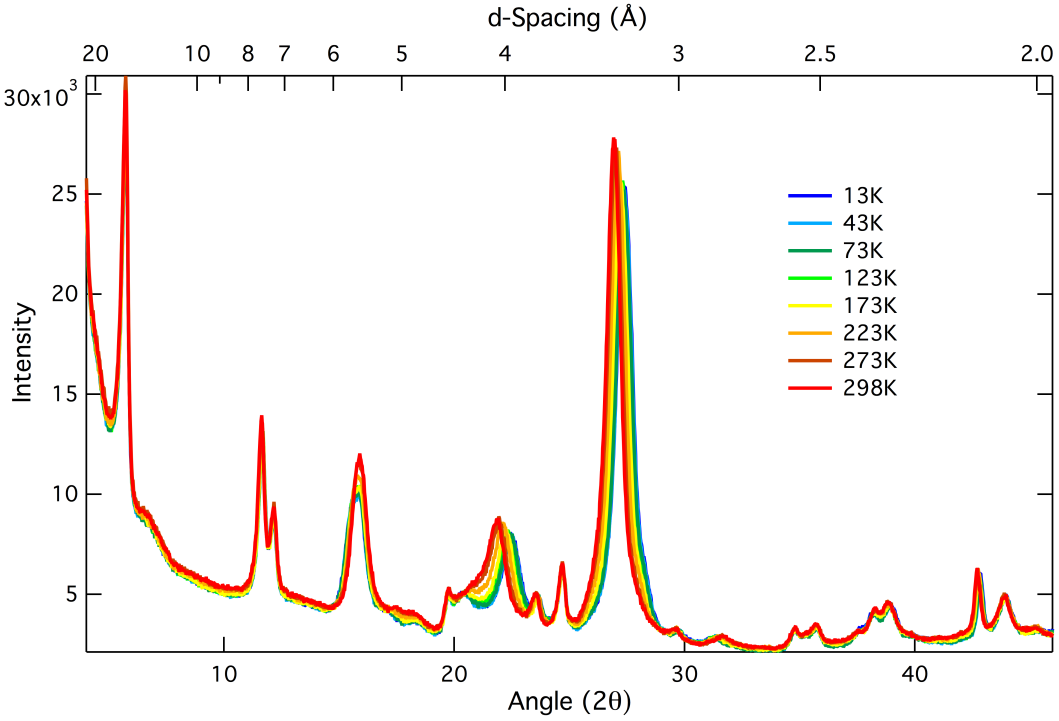

Figure 1 Temperature dependent PXRD of β-QA at eight temperatures in the range 13–298 K.

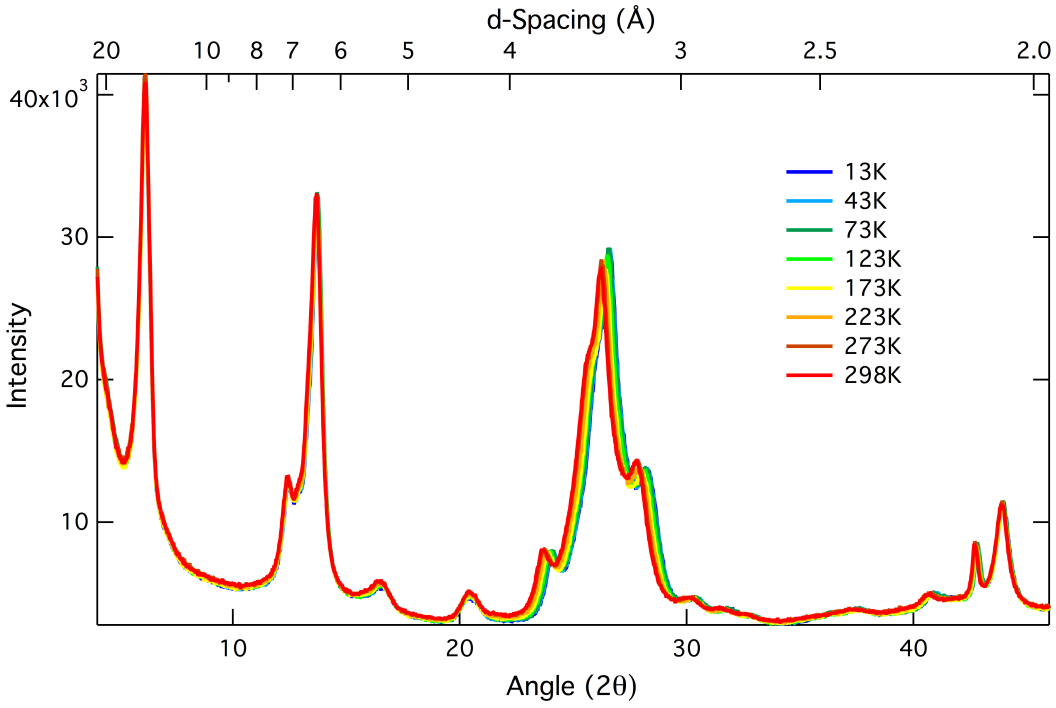

Figure 2 Temperature dependent PXRD of of γ-QA at eight temperatures in the range 13–298 K.

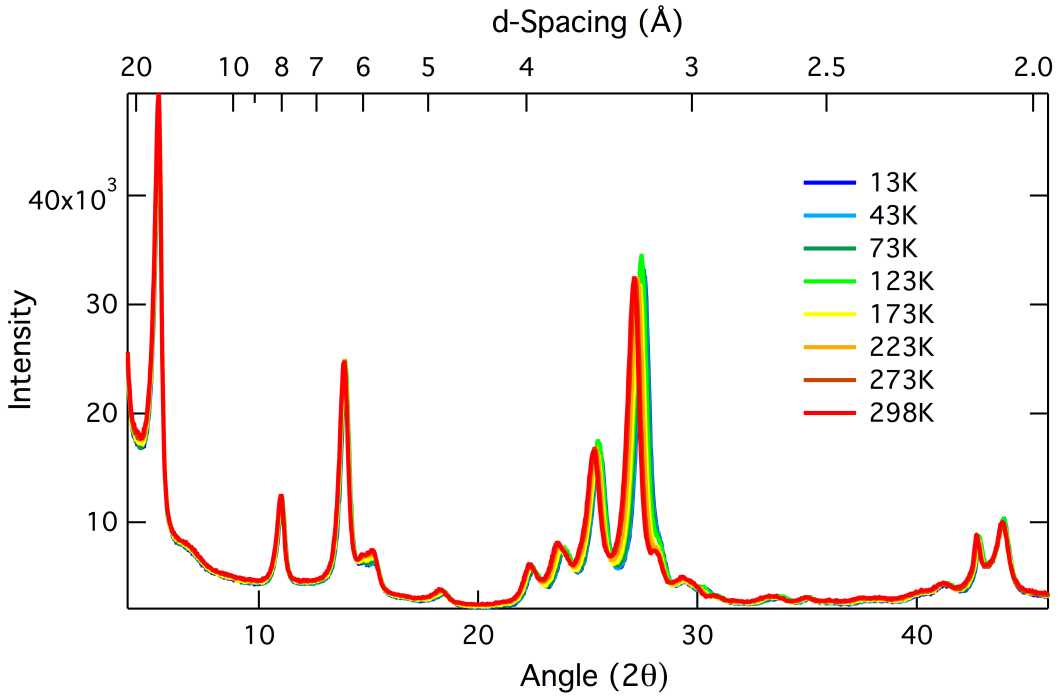

Figure 3 Temperature dependent PXRD of 2,9-DMQA at eight temperatures in the range 13–298 K.

1.2 Spectroscopy

This section provides the full THz spectroscopy temperature measurements made from 20–300 K on the quinacridone solids. Subsequently, fitted positions and amplitudes for each labelled peak are provided

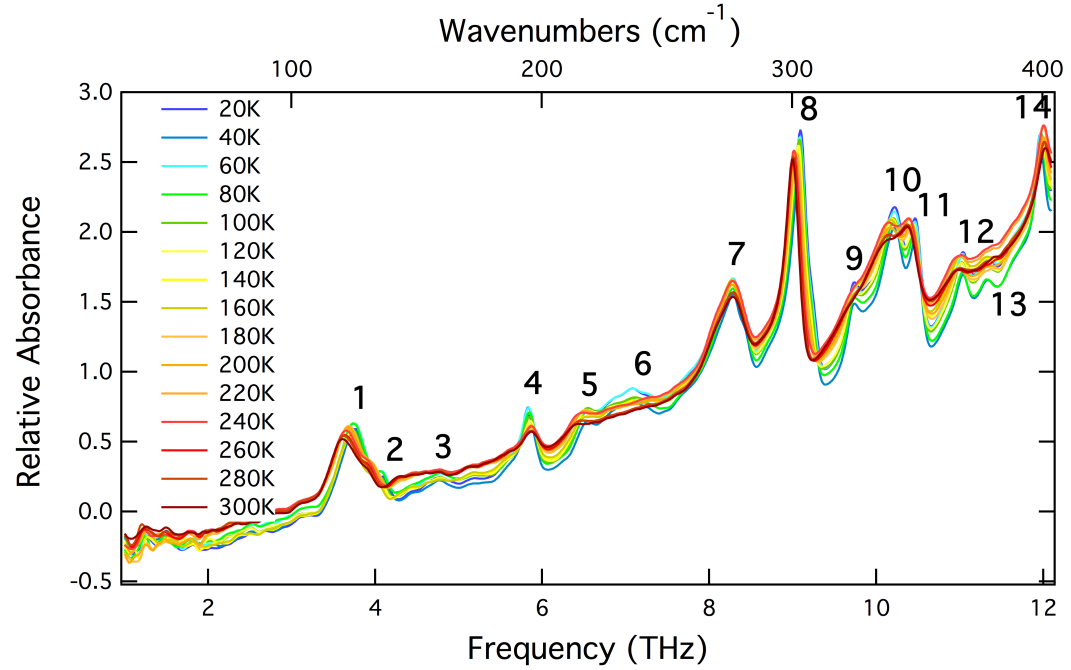

Figure 4 Temperature dependent THz spectroscopy of β-QA in the range 20–300 K.

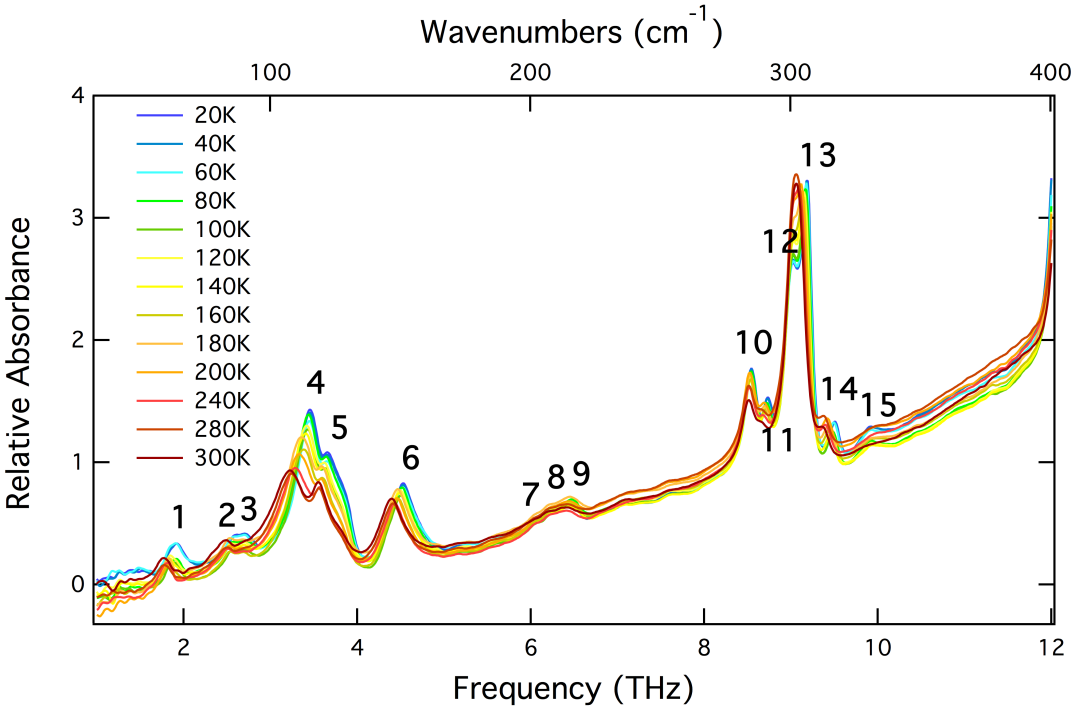

Figure 5 Temperature dependent THz spectroscopy of γ-QA in the range 20–300 K.

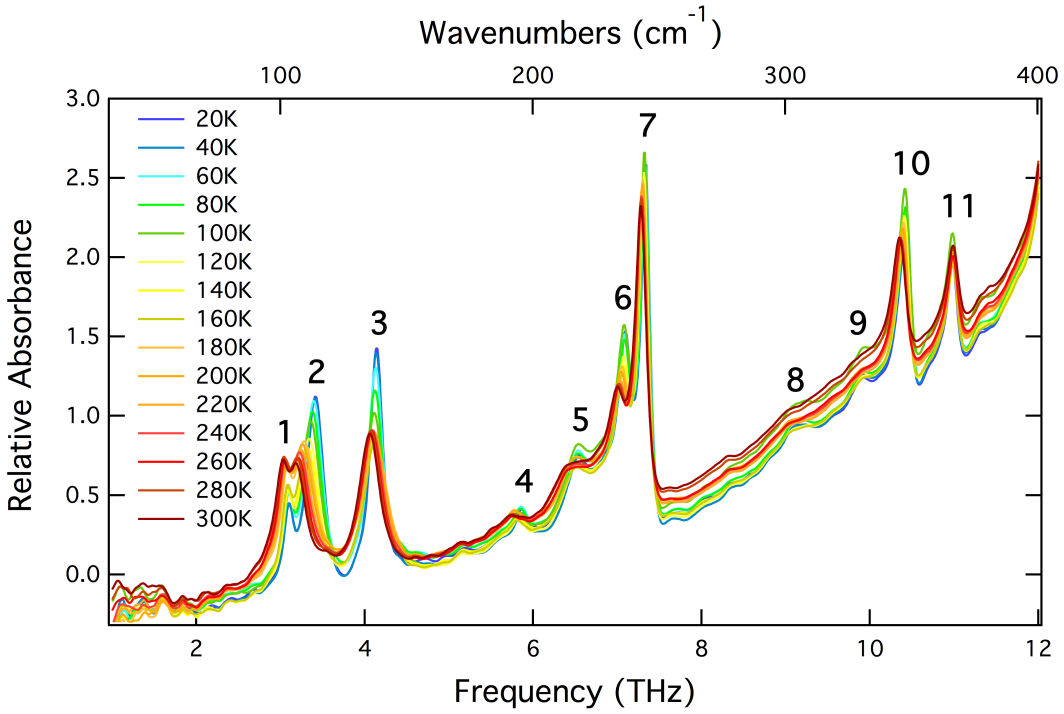

Figure 6 Temperature dependent THz spectroscopy of 2,9-DMQA in the range 20–300 K.

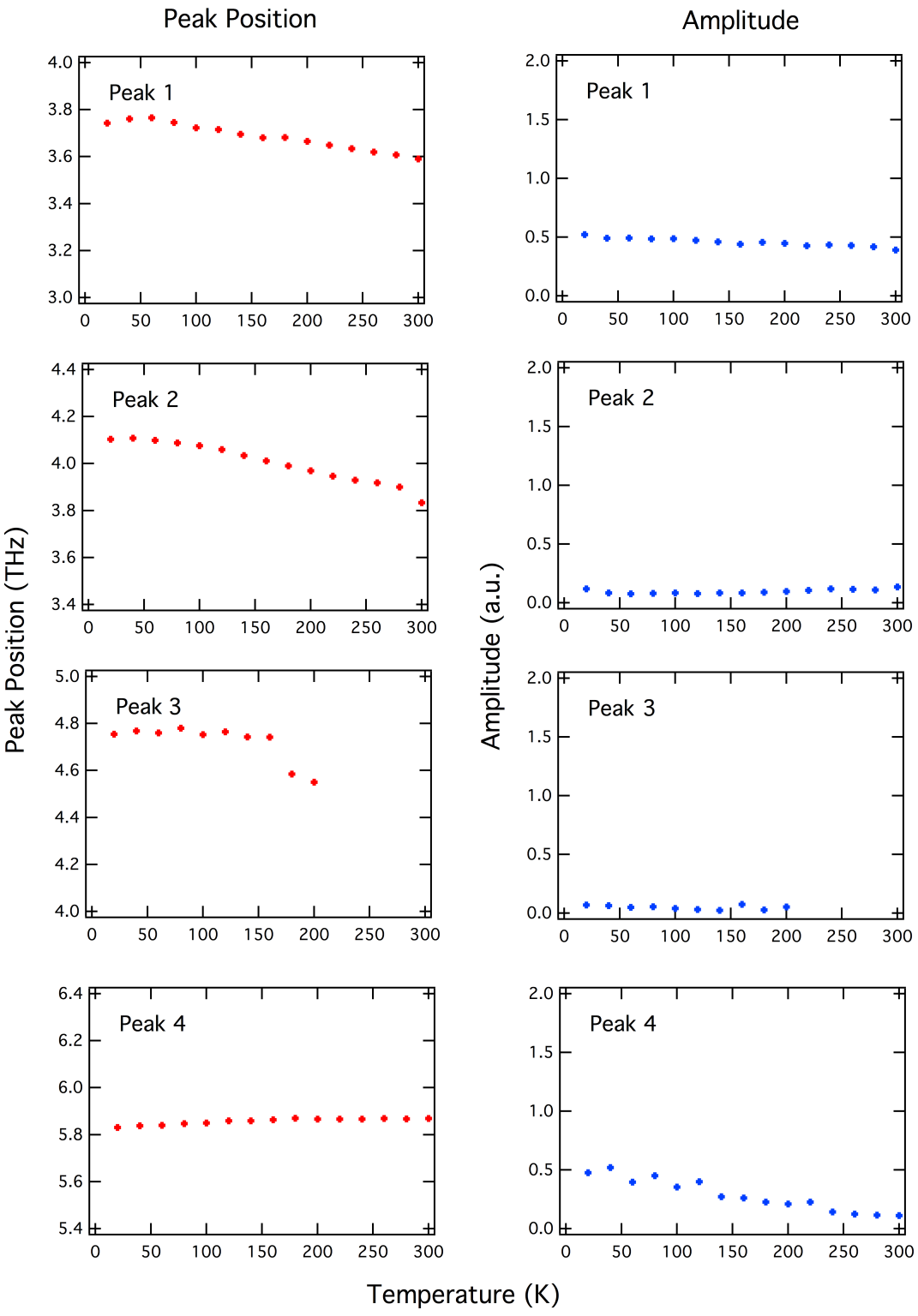

Figure 7 Temperature dependence of position and amplitude for vibrational modes in β-QA from 3–6 THz.

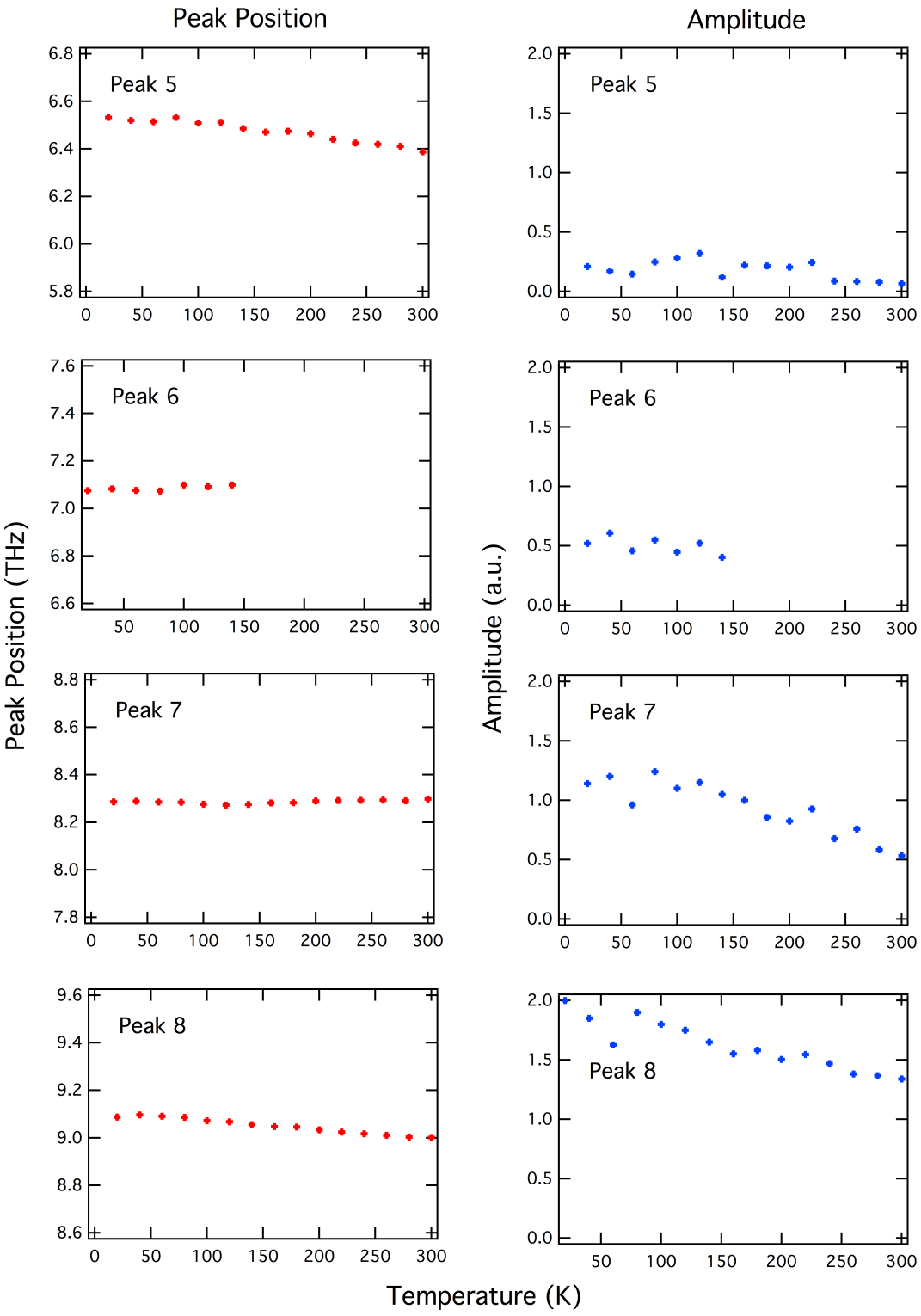

Figure 8 Temperature dependence of position and amplitude for vibrational modes in β-QA from 6–9 THz.

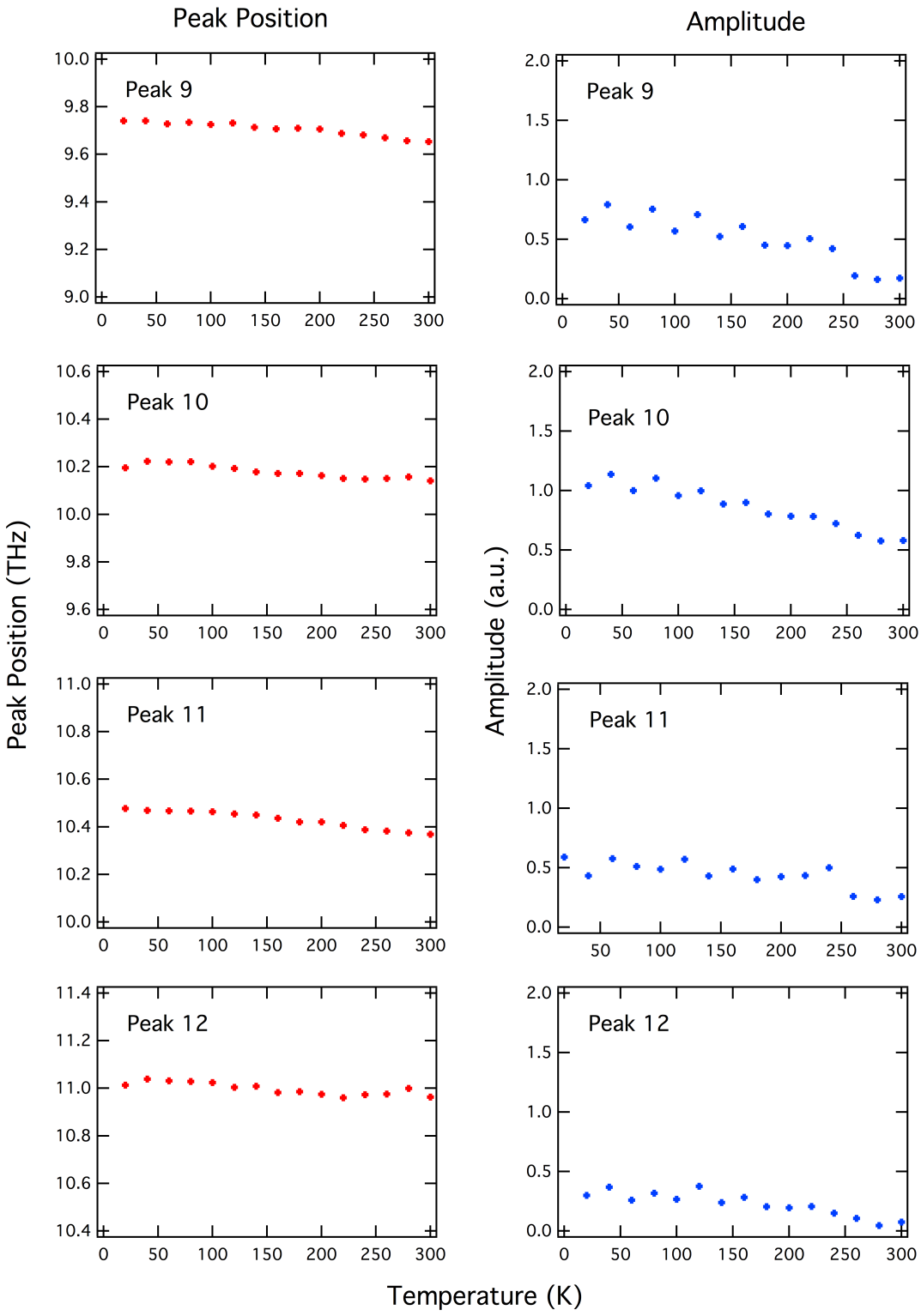

Figure 9 Temperature dependence of position and amplitude for vibrational modes in β-QA from 9–11 THz.

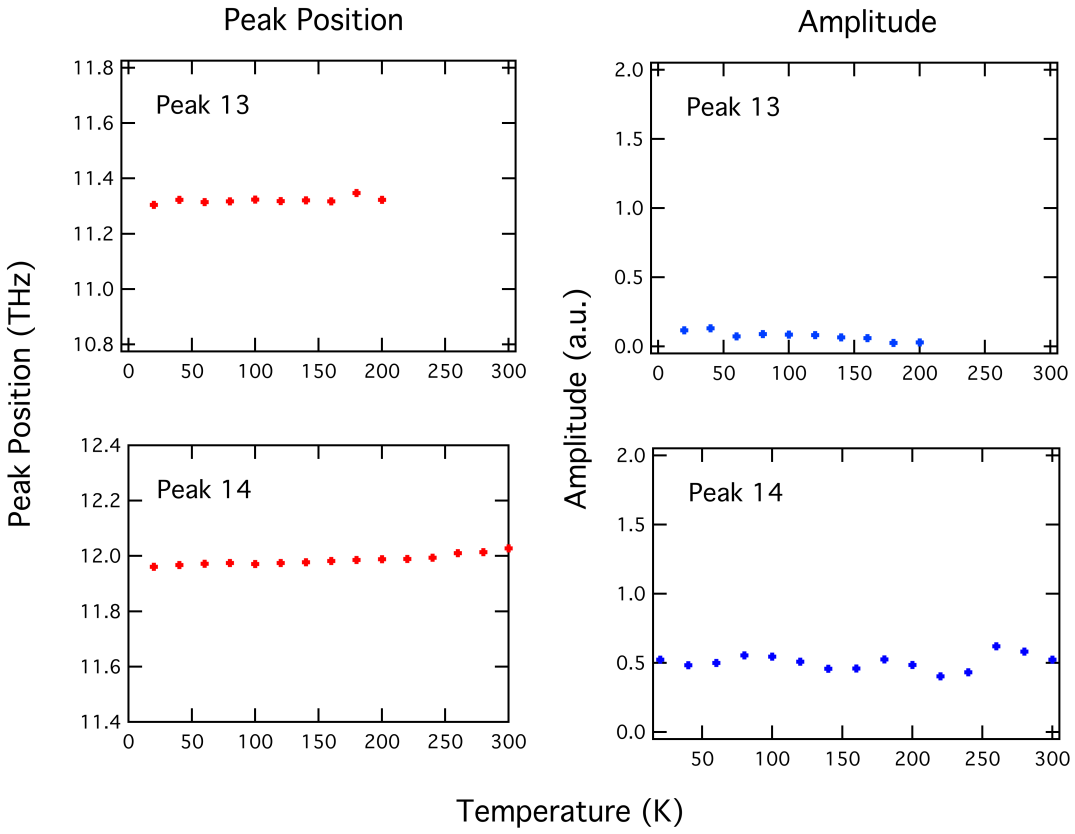

Figure 10 Temperature dependence of position and amplitude for vibrational modes in β-QA from 11–12 THz.

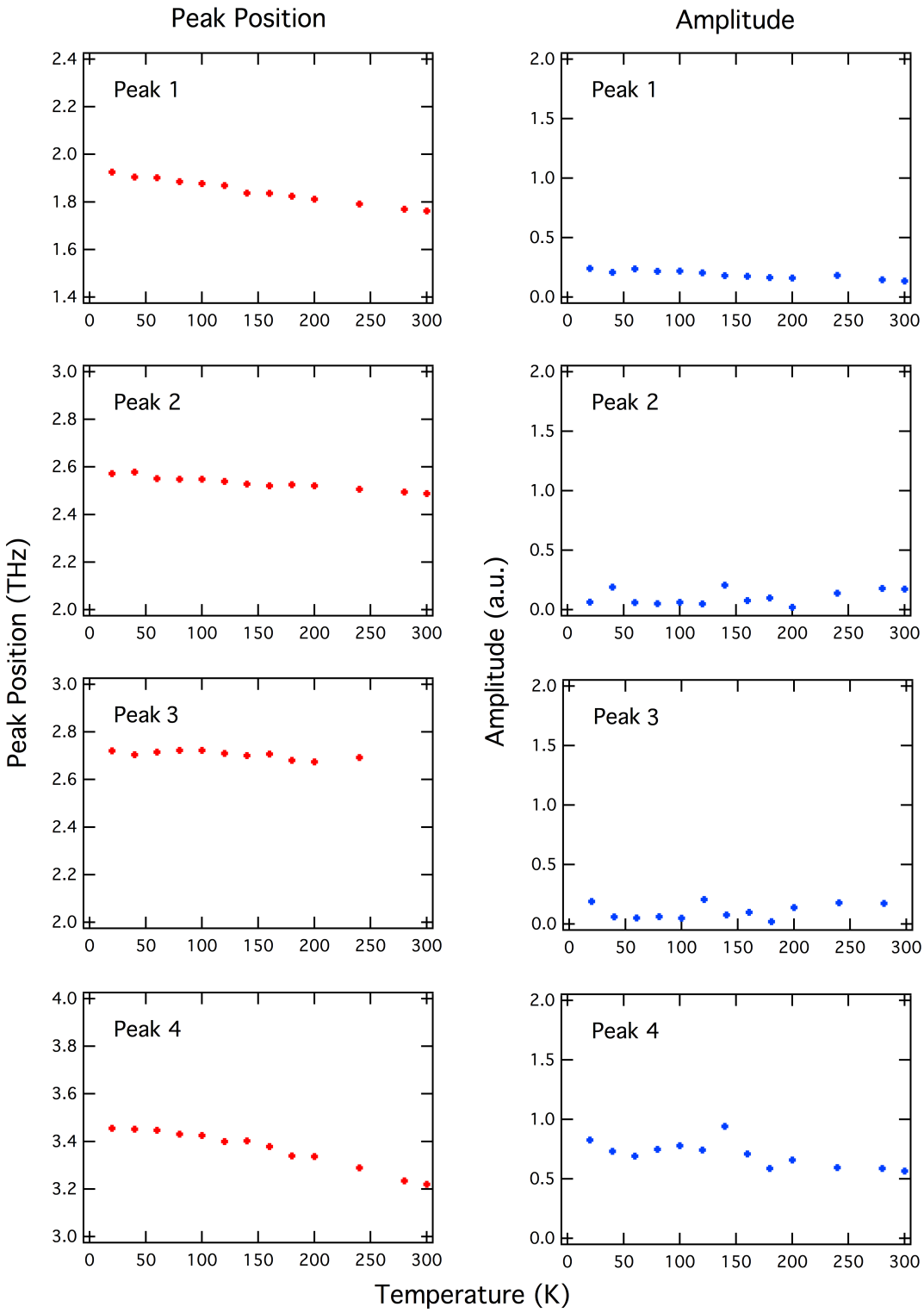

Figure 11 Temperature dependence of position and amplitude for vibrational modes in γ-QA from 2–3.5 THz.

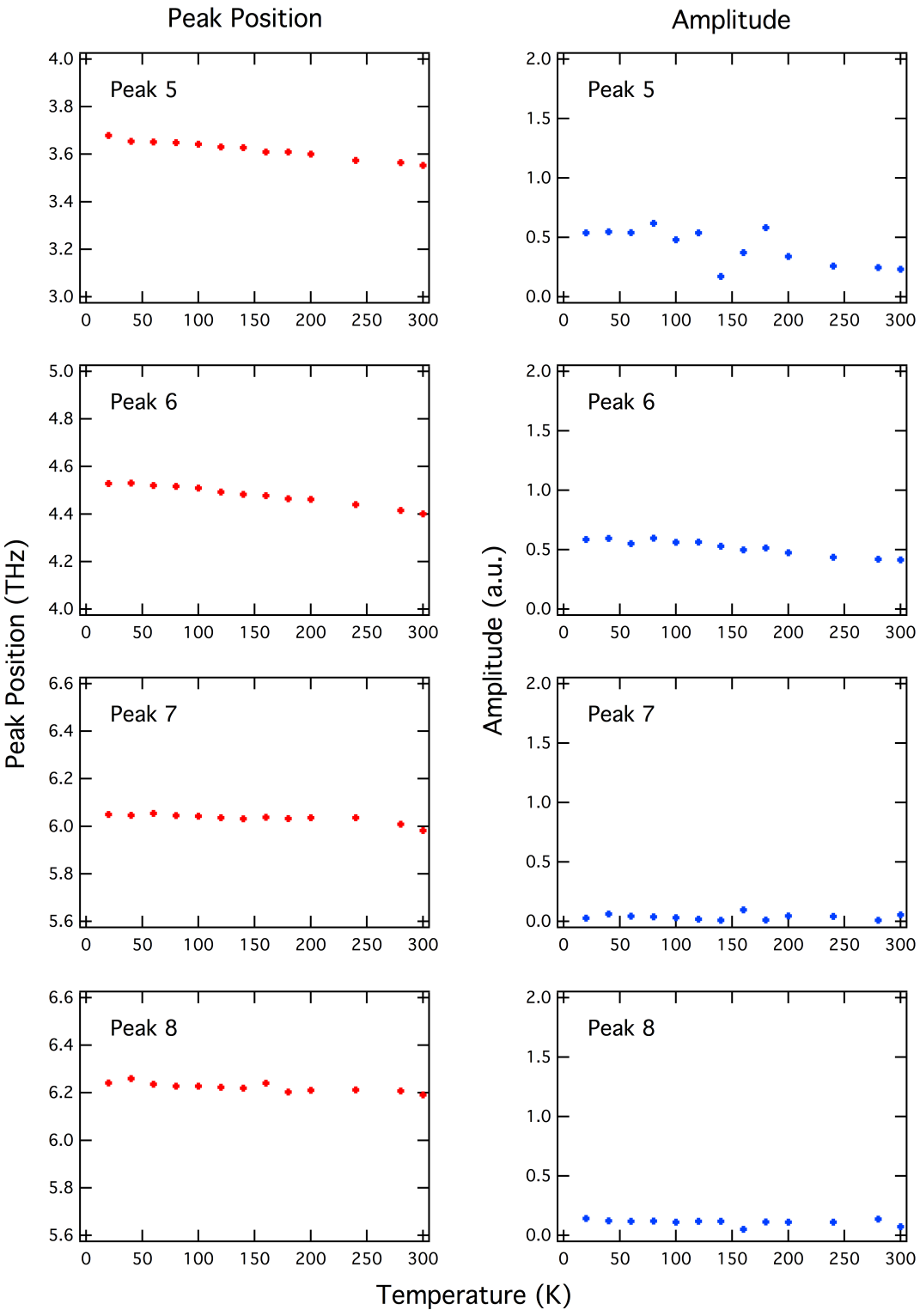

Figure 12 Temperature dependence of position and amplitude for vibrational modes in γ-QA from 3.5–6.5 THz.

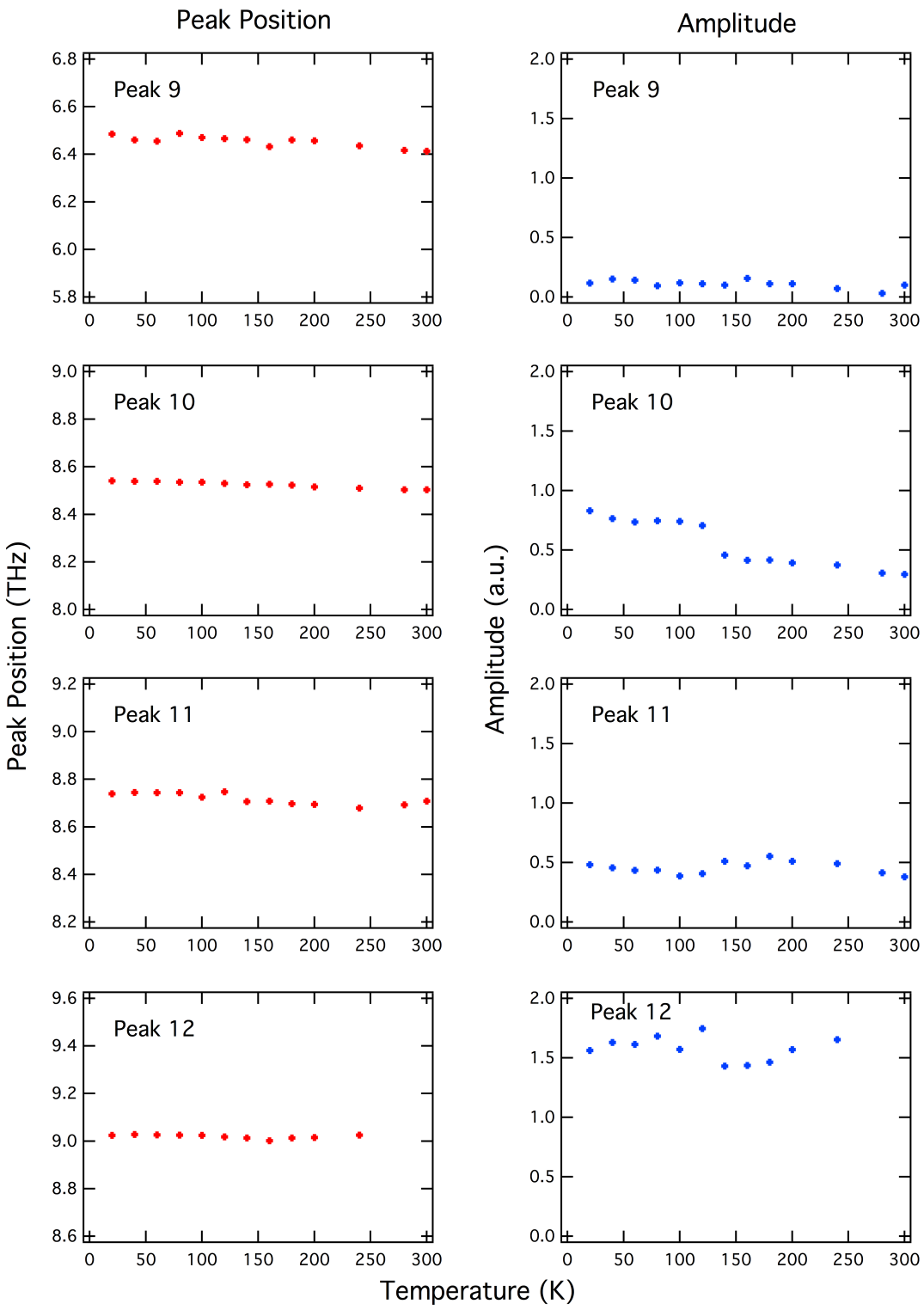

Figure 13 Temperature dependence of position and amplitude for vibrational modes in γ-QA from 6.5–9 THz.

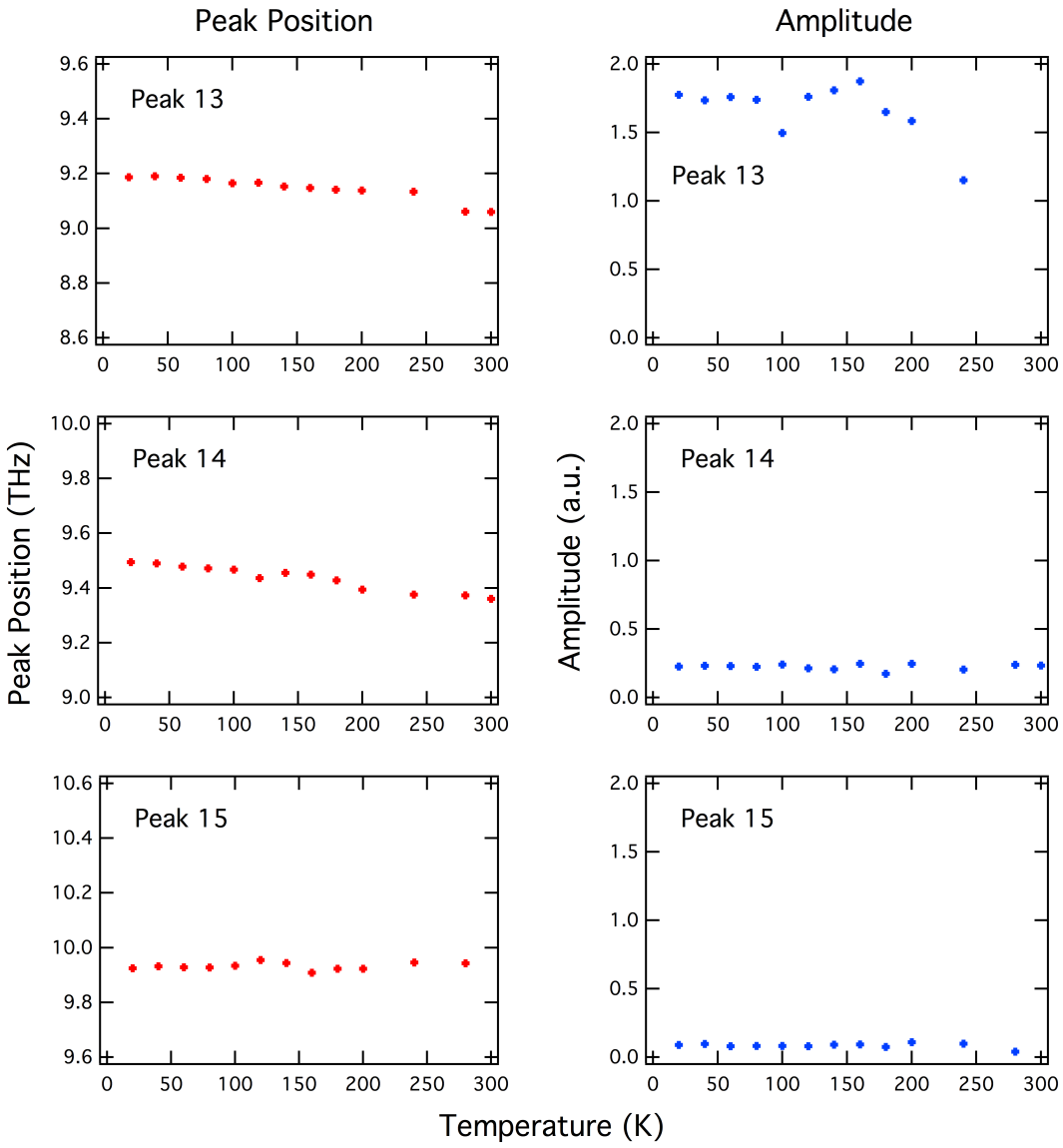

Figure 14 Temperature dependence of position and amplitude for vibrational modes in γ-QA from 9–11 THz.

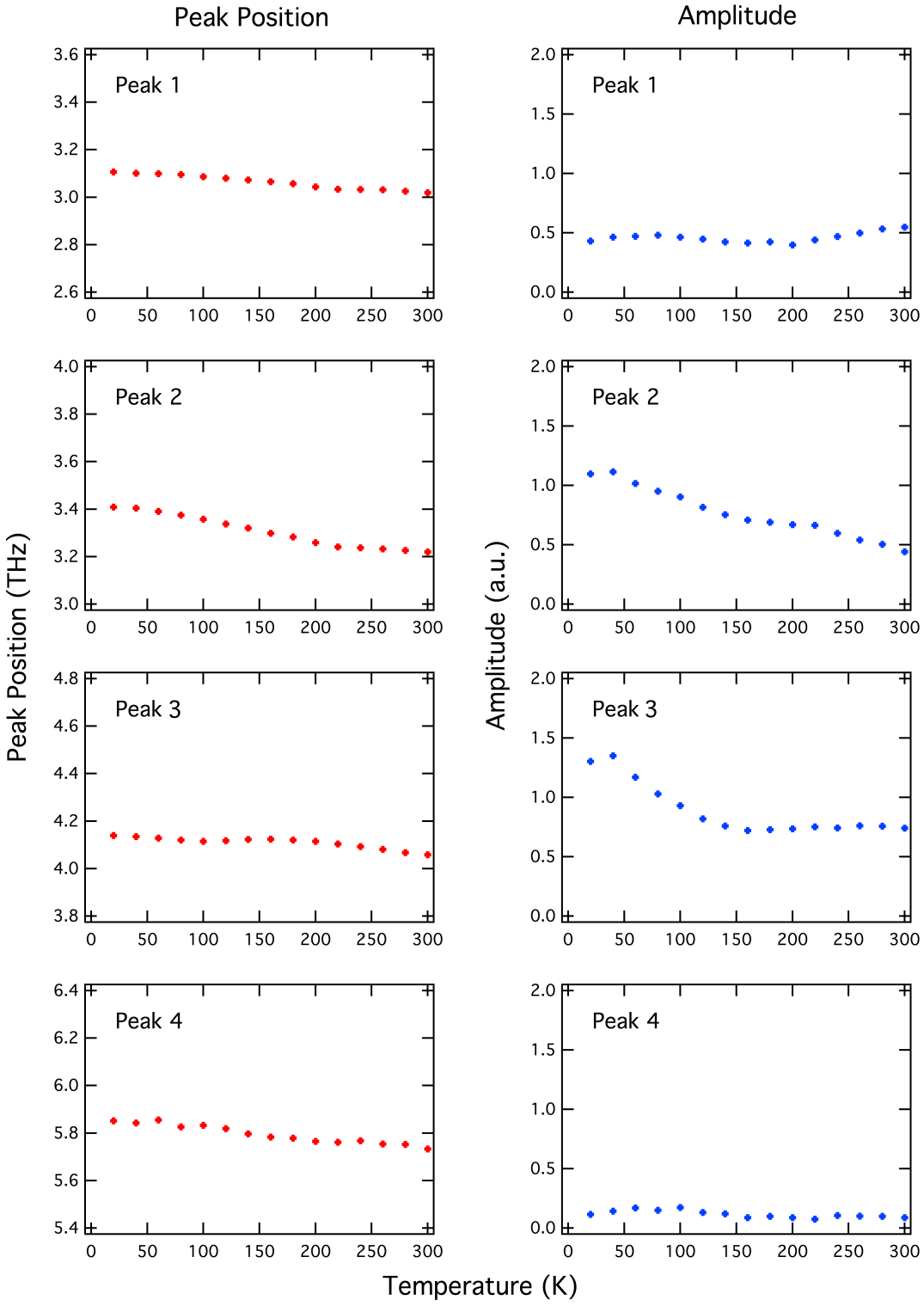

Figure 15 Temperature dependence of position and amplitude for vibrational modes in 2,9-DMQA from 3–6 THz.

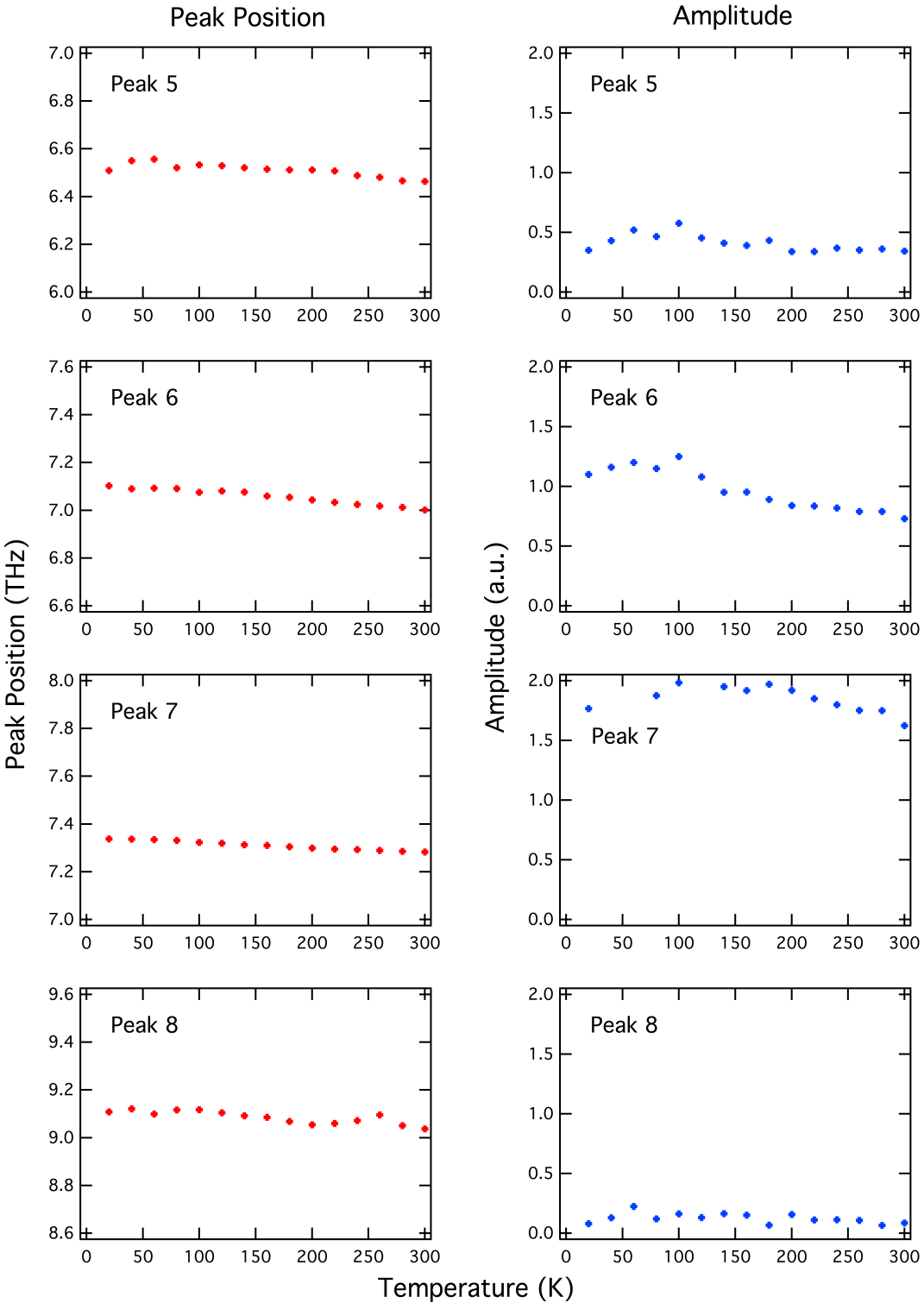

Figure 16 Temperature dependence of position and amplitude for vibrational modes in 2,9-DMQA from 6–9.5 THz.

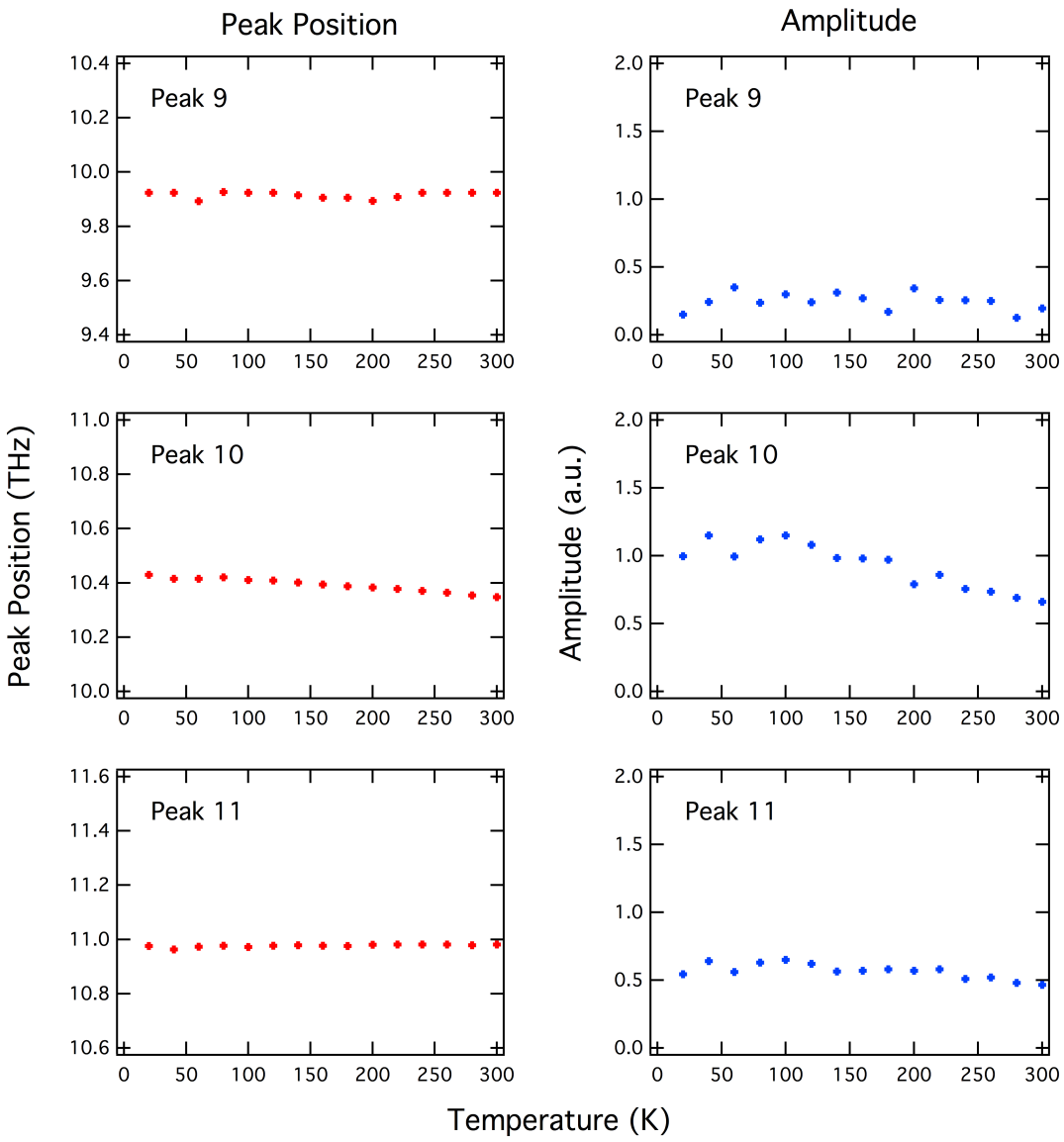

Figure 17 Temperature dependence of position and amplitude for vibrational modes in 2,9-DMQA from 9.5–11 THz.

1.3 Position comparison with SS-DFT

This section provides comparison of fitted peak positions with corresponding modes from DFT modelling. Summary tables and detailed analysis on the peak/mode assignment for each quinacridone solid is given.

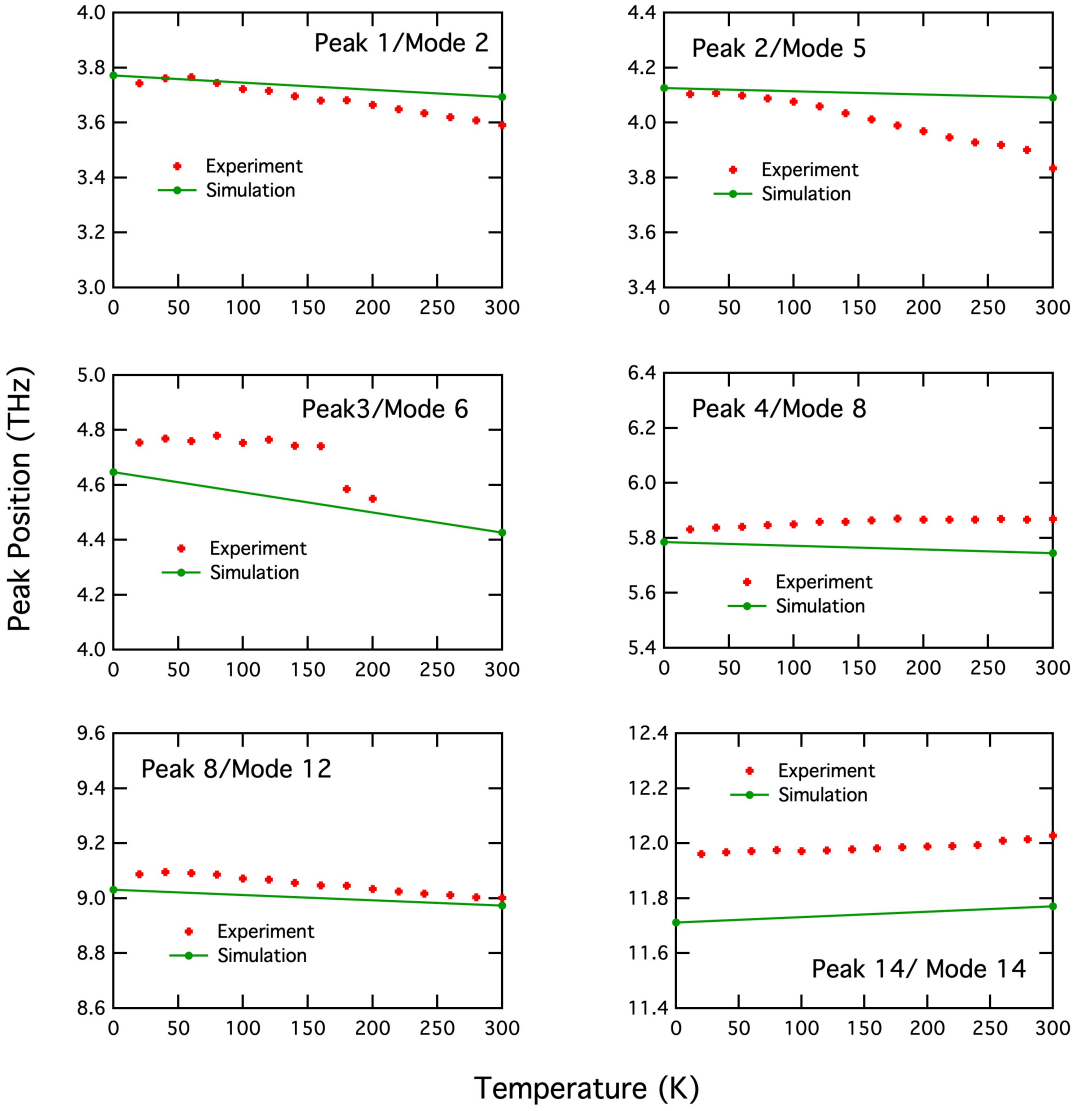

Figure 18 Experiment and simulation of change of energy with temperature for β-QA. Simulated data (green) corresponds to a volume expansion of 2% from 0–300 K. The vertical range of each panel is set at 1 THz for ease of comparison.

Table 1 β-QA features as determined by experiment and fully optimized simulated structures.

Experiment			Simulation			Comment
Peak Label	Frequency (THz)	Wavenumber (cm^{-1})	Mode Label	Frequency (THz)	Wavenumber (cm^{-1})	
N/A			1	2.70	90	not observed, weak
1	3.74	125	2	3.63	121	
N/A			3	3.89	130	likely unresolved with Peak 1
N/A			4	4.08	136	likely unresolved with Peak 2
2	4.10	137	5	4.12	138	
3	4.75	159	6	4.39	146	observed below 220 K
N/A			7	5.17	172	not observed
4	5.83	195	8	5.77	192	
N/A			9	6.30	210	not observed, very weak
5	6.53	218	N/A			not in model
6	7.08	236	N/A			observed below 160 K, not in model
7	8.29	276	N/A			not in model
N/A			10	8.48	283	not observed, very weak
N/A			11	8.69	290	likely unresolved with Peak 8
8	9.09	303	12	9.02	301	
N/A			13	9.05	302	likely unresolved with Peak 8
9	9.74	325	N/A			not in model
10	10.20	340	N/A			not in model
11	10.48	349	N/A			not in model
12	11.01	367	N/A			not in model
13	11.30	377	N/A			observed below 220 K, not in model
14	11.96	399	14	11.67	389	

Three peaks from 6.5–8.5 THz and five from 9.5–11.5 THz are observed experimentally which are not reflected in the simulated data. These are likely due to the presence of impurities or additional phases, consistent with PXRD data, which break down the strict selection rules employed in simulation. Likewise, a series of predicted modes are also not present in experimental results. Mode 1 is weak and only prominent in a 2% contraction. At the limit of the experimental setup, it is unlikely that this feature could be resolved. Modes 3 and 4 are positioned very close to the experimental Peaks 1 and 2. These are probably unresolved with these peaks, as evidenced by asymmetry, particularly in the high frequency shoulder of Peak 1. Mode 7 is not observed experimentally, with this result remaining unclear. Modes 9 and 10 are presumably too weak for observation. Modes 11 and 13 are situated very close to the large, characteristic Peak 8. With their significantly lower amplitude these features cannot be resolved. Convolved simulated spectra in Fig. 7 in the main text also fail to definitively show these modes. A low temperature asymmetry in the low frequency shoulder of Peak 8 gives evidence of Mode 11.

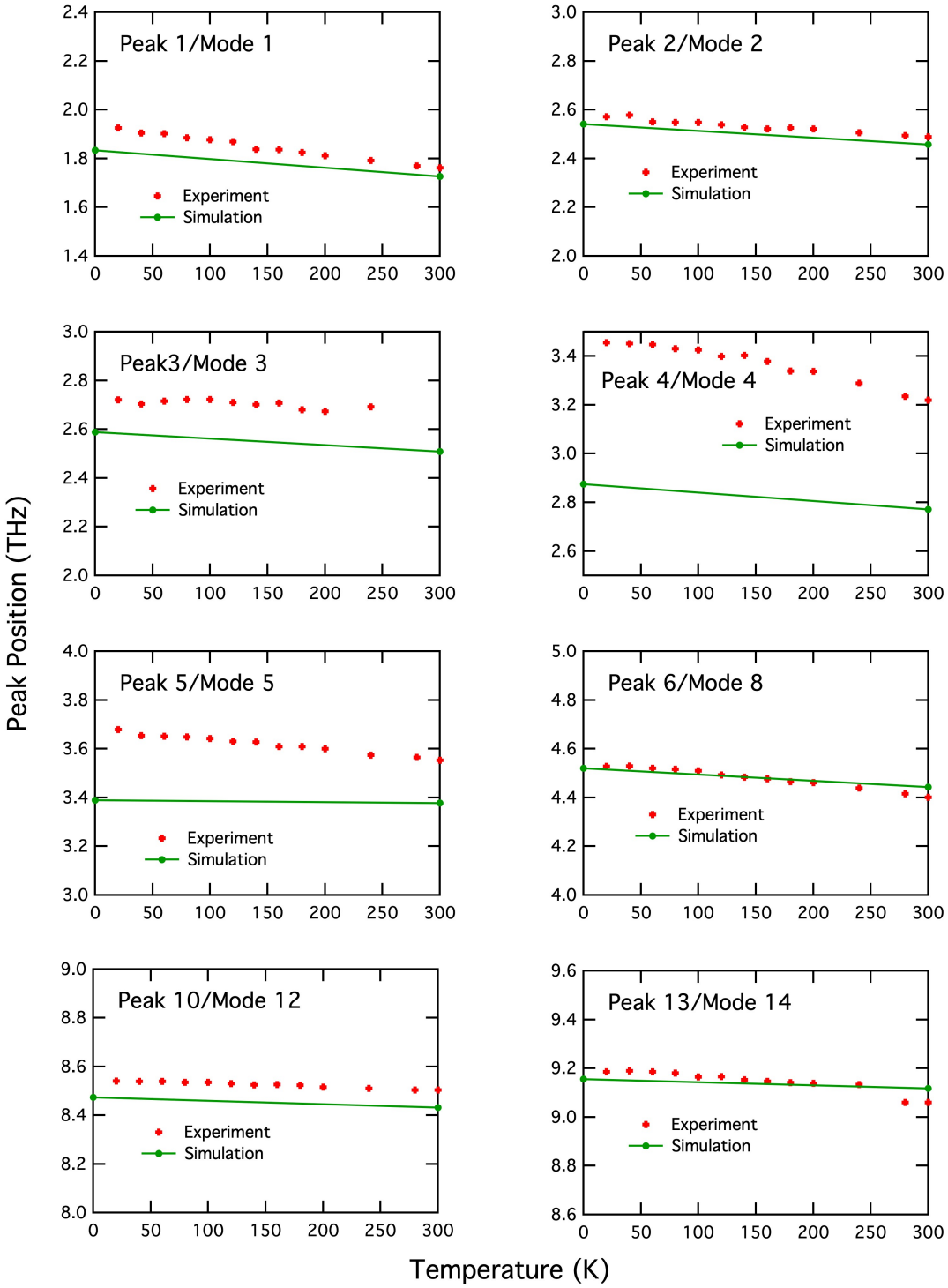

Figure 19 Experiment and simulation of change of energy with temperature for γ-QA. Simulated data (green) corresponds to a volume expansion of 2% from 0–300 K. The vertical range of each panel is set at 1 THz for ease of comparison.

Table 2 γ-QA features as determined by experiment and fully optimized simulated structures.

Experiment			Simulation			Comment
Peak Label	Frequency (THz)	Wavenumber (cm^{-1})	Mode Label	Frequency (THz)	Wavenumber (cm^{-1})	
1	1.93	64	1	1.83	61	
2	2.57	86	2	2.54	85	
3	2.72	91	3	2.59	86	below 240 K
4	3.46	115	4	2.87	96	
5	3.68	123	5	3.39	113	
N/A			6	3.86	129	likely unresolved with Peak 5
N/A			7	3.91	130	likely unresolved with Peak 5
6	4.53	151	8	4.52	151	
N/A			9	4.74	158	not observed
7	6.05	202	10	6.16	205	
8	6.24	208	N/A			not in model
9	6.49	216	N/A			not in model
N/A			11	6.65	222	not observed
10	8.54	285	12	8.47	283	
11	8.74	292	13	8.61	287	
12	9.02	301	N/A			below 240 K, not in model
13	9.19	306	14	9.16	305	
14	9.49	317	15	9.50	317	
15	9.92	331	N/A			below 280 K, not in model

In γ-QA, Peaks 8, 9, 12, and 15 are observed experimentally but not generated in simulations. It is hypothesized that these are due to sample impurities and crystal defects, which would violate selection rules for allowed transitions in the simulation method. Modes 6, 7, 9, and 11 are predicted by theory but are not observed experimentally. Modes 6 and 7 are weak and are very closely spaced to each other and to Peak 5. It is probable that these modes are present in the high frequency shoulder of Peak 5 as evidenced by its asymmetric profile. Modes 9 and 11 are very weak and likely cannot be observed with the employed experimental method.

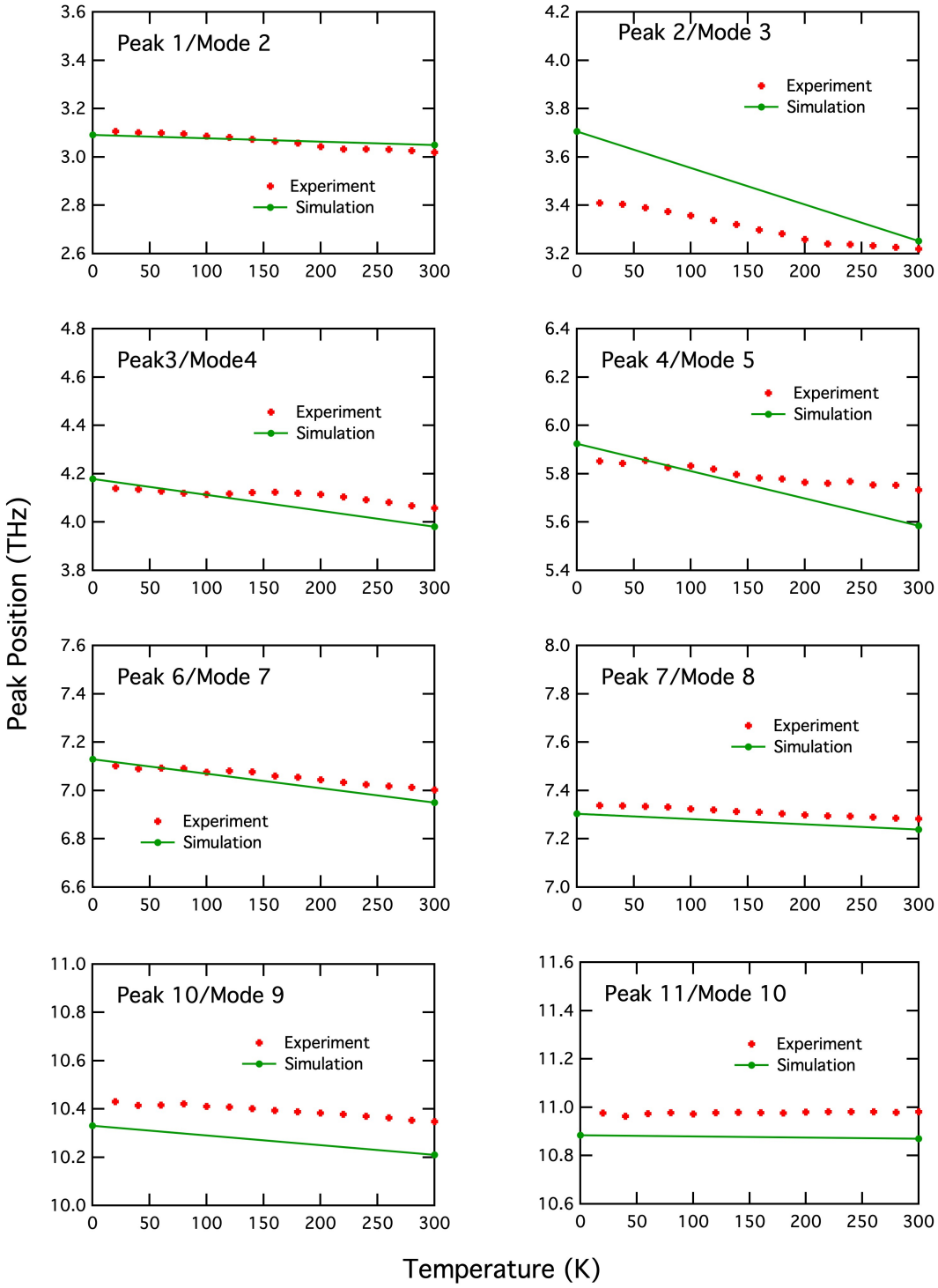

Figure 20 Experiment and simulation of change of energy with temperature for 2,9-DMQA. Simulated data (green) corresponds to a volume expansion of 4% from 0–300 K. The vertical range of each panel is set at 1 THz for ease of comparison.

Table 3 2,9-DMQA features as determined by experiment and fully optimized simulated structures.

Experiment			Simulation			Comment
Peak Label	Frequency (THz)	Wavenumber (cm^{-1})	Mode Label	Frequency (THz)	Wavenumber (cm^{-1})	
0	1.52	51	1	1.58	52	
1	3.02	101	2	3.09	103	
2	3.22	107	3	3.70	124	
3	4.06	135	4	4.18	139	
N/A			5	5.06	169	not observed
4	5.73	191	6	5.92	198	
5	6.46	215	N/A			not in model
6	7.00	233	7	7.13	238	
7	7.28	243	8	7.30	244	
8	9.04	301	N/A			not in model
9	9.92	331	N/A			not in model
10	10.35	345	9	10.33	345	
11	10.98	366	10	10.88	363	

Some of the peaks observed in experiment for 2,9-DMQA do not appear in the simulation. These include the experimental peaks labelled 5, 8, and 9. The origin of these additional experimental peaks is not certain. They may arise from impurities in the crystal. They may also arise from defects in the crystal, which break the strict dipole selection rules employed in the simulation to determine the allowed transitions. Likewise, one of the calculated modes, labelled 5, is not observed in the experiment. The mode is probably too weak for observation under the experimental conditions employed.

1.4 Amplitude comparison with SS-DFT

This section provides comparison of fitted peak amplitudes with corresponding modes from DFT modelling.

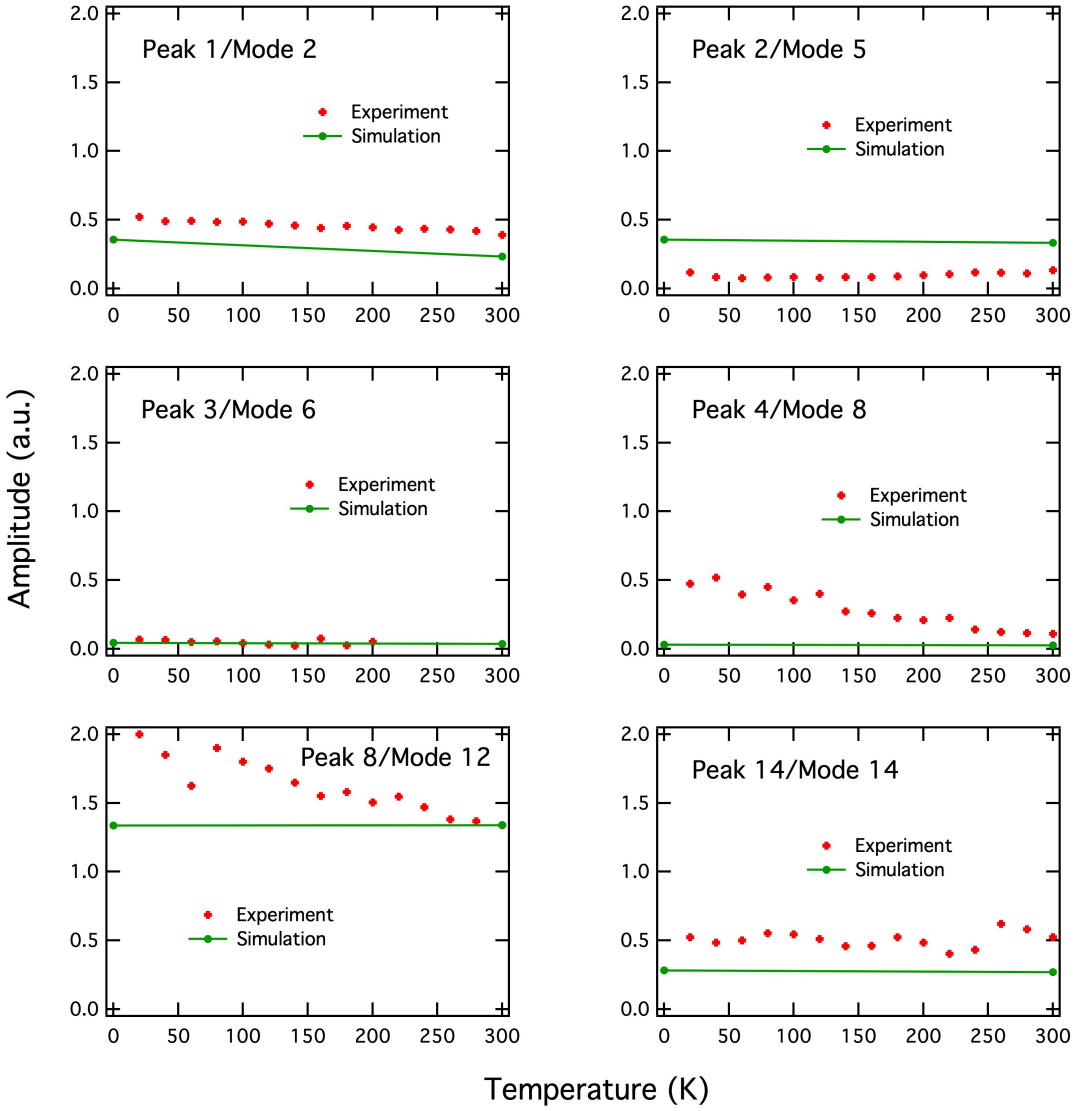

Figure 21 Experiment and simulation of change amplitude with temperature for β-QA. The vertical range of each panel is set at 2.0 for ease of comparison. The (green) line with two points simulates absolute zero with no volume change and 300 K with a $+2$% expansion.

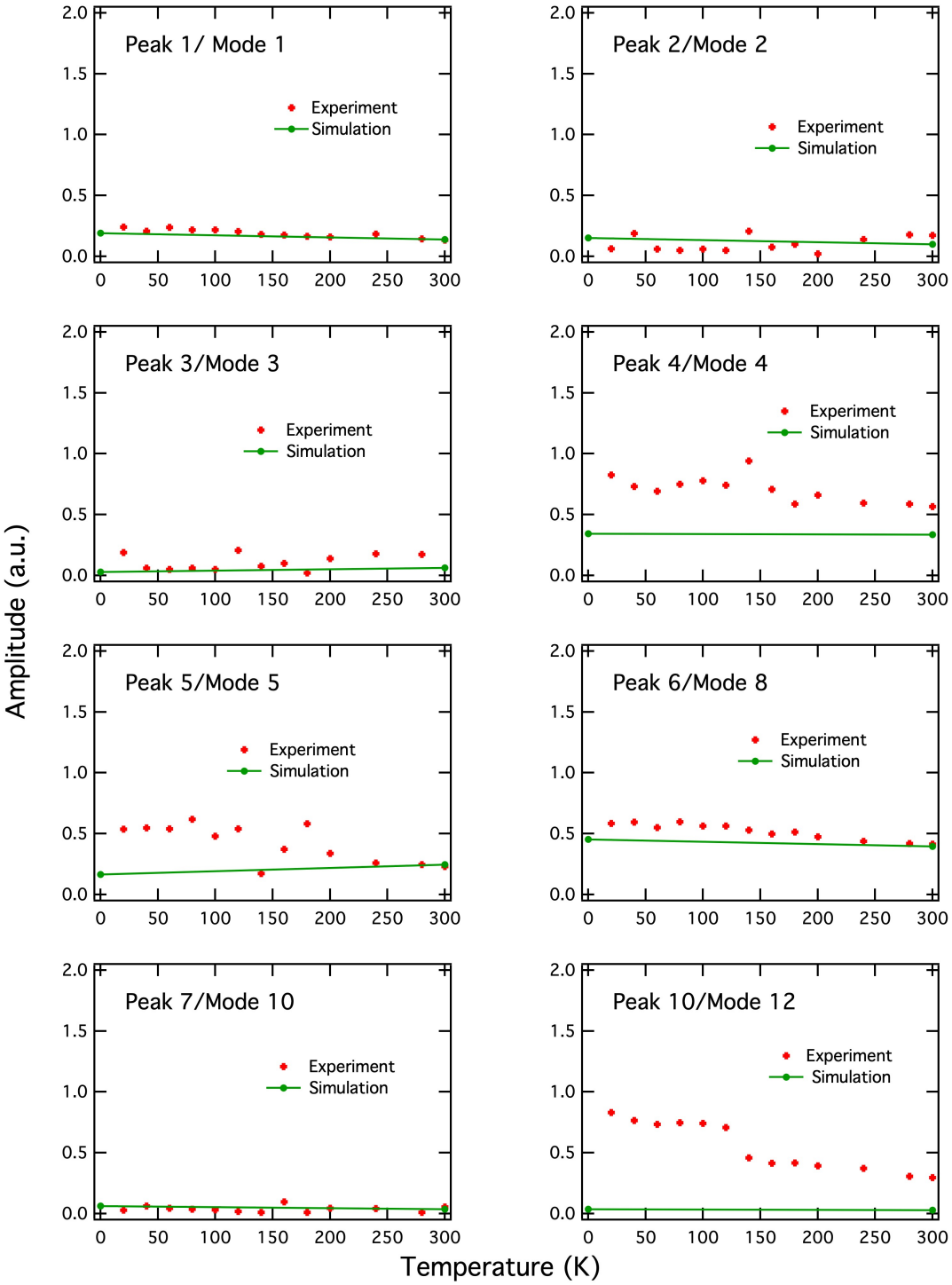

Figure 22 Experiment and simulation of change amplitude with temperature for γ-QA. The vertical range of each panel is set at 2.0 for ease of comparison. The (green) line with two points simulates absolute zero with no volume change and 300 K with a $+2$% expansion.

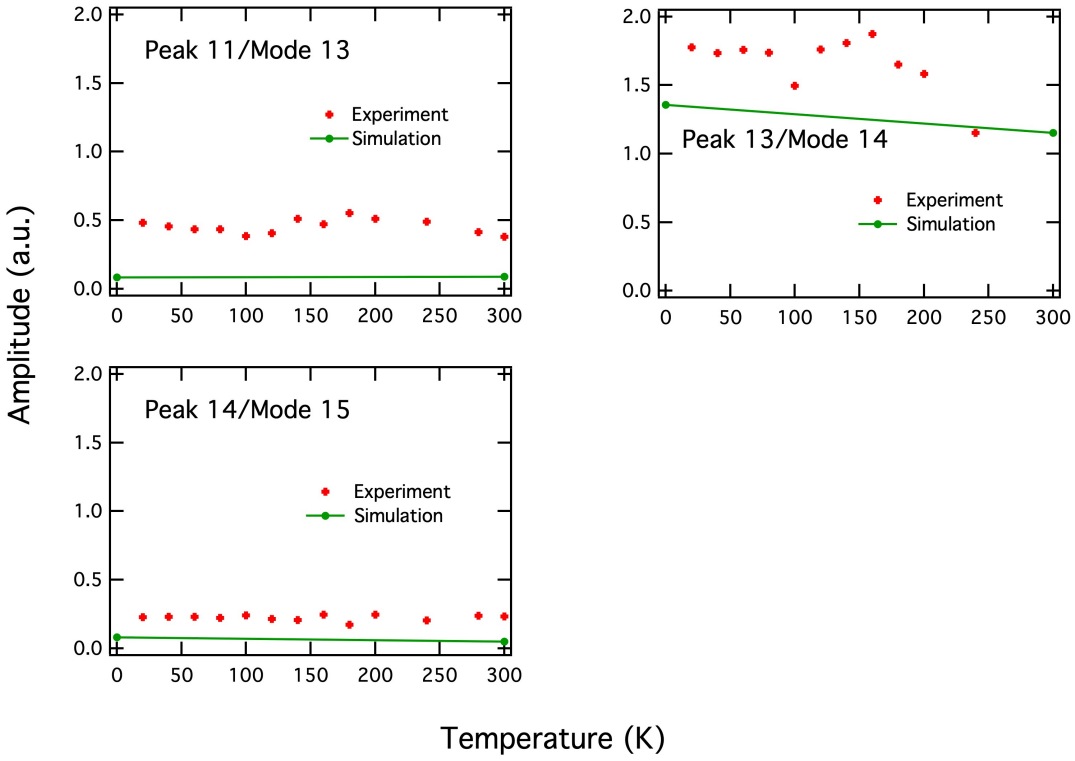

Figure 23 Experiment and simulation of change amplitude with temperature for γ-QA. The vertical range of each panel is set at 2.0 for ease of comparison. The (green) line with two points simulates absolute zero with no volume change and 300 K with a $+2\%$ expansion.

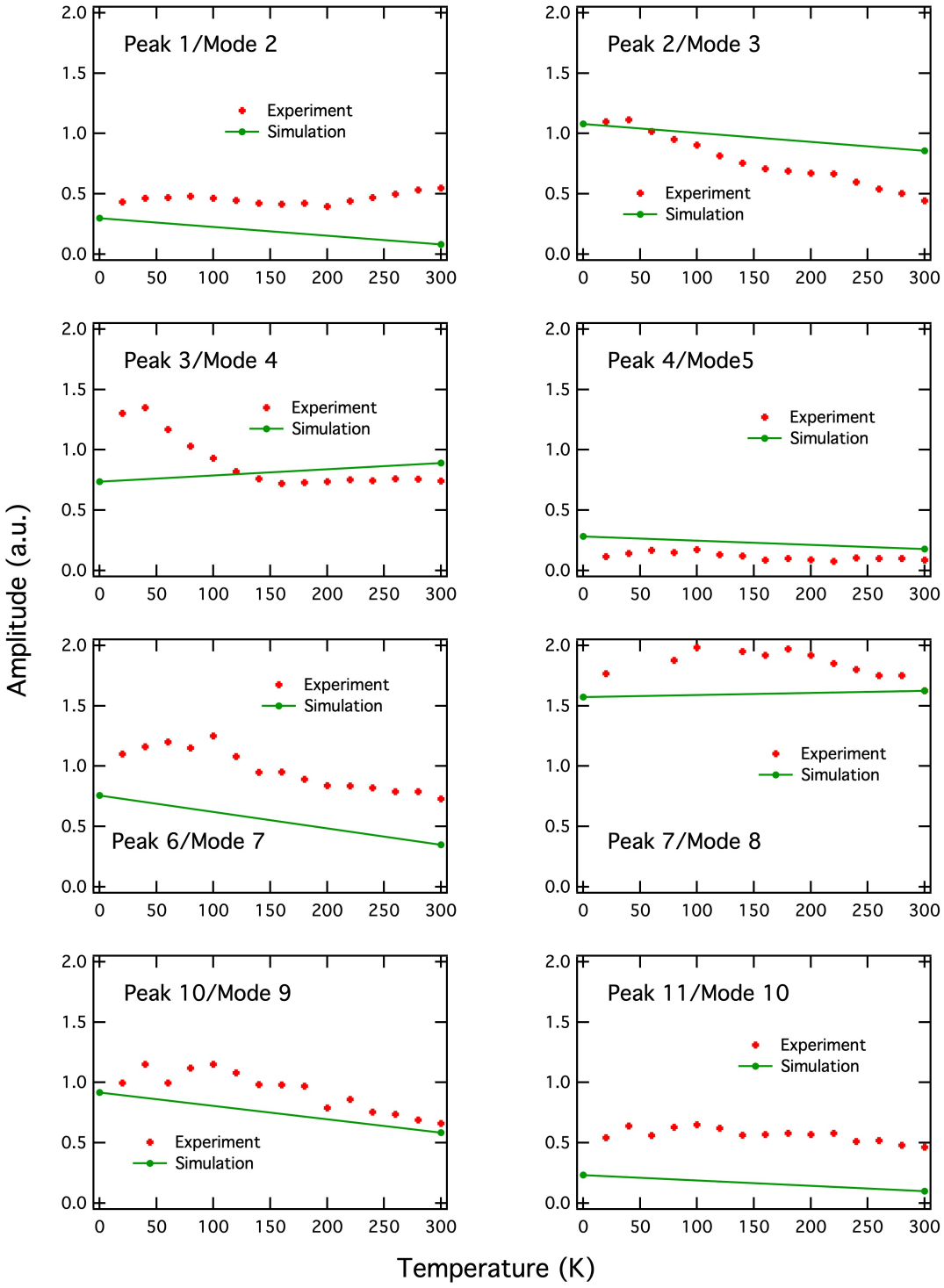

Figure 24 Experiment and simulation of change amplitude with temperature for 2,9-DMQA. The vertical range of each panel is set at 2.0 for ease of comparison. The (green) line with two points simulates absolute zero with no volume change and 300 K with a +2% expansion.